Available online at www.sciencedirect.com

SCIENCE DIRECT®

International Journal of Mass Spectrometry 228 (2003) 117–126

International Journal of Mass Spectrometry

www.elsevier.com/locate/ijms

Selected ion flow tube, SIFT, studies of the reactions of H_3O^+, NO^+ and $O_2{}^+$ with eleven $C_{10}H_{16}$ monoterpenes

Tianshu Wang[a], Patrik Španěl[b], David Smith[a,*]

[a] *Centre for Science and Technology in Medicine, School of Medicine, Keele University,*
Thornburrow Drive, Hartshill, Stoke-on-Trent ST4 7QB, UK
[b] *V. Čermák Laboratory, J. Heyrovský Institute of Physical Chemistry, Academy of Sciences of the Czech Republic,*
Dolejškova 3, 182 23, Prague 8, Czech Republic

Received 24 April 2003; accepted 26 May 2003

Abstract

The reactions of H_3O^+, NO^+ and $O_2{}^+$ have been studied with the 11 terpenes, myrcene, ocimene, α- and β-pinene, α- and γ-terpinene, 2- and 3-carene, *R*- and *S*-limonene and camphene, at thermal energies using a selected ion flow tube (SIFT). This study was intended to explore the potential of SIFT mass spectrometry (SIFT-MS), for analysing terpenes in air. All 33 reactions are seen to proceed at the collisional rate and multiple product ions result. The H_3O^+ reactions result in two major ion products, the stable protonated terpenes $C_{10}H_{17}{}^+$ together with $C_6H_9{}^+$ ions, with some minor products (a few percent) in some reactions. The NO^+ reactions result in the parent cations, $C_{10}H_{16}{}^+$, as the major product ion together with several fragment ions, notable $C_7H_9{}^+$. The appearance of the minority adducts H_3O^+M and NO^+M provide clues to the mechanisms of these reactions. The more energetic $O_2{}^+$ ions result in greater fragmentation and the parent terpene cations are only minority products. We conclude that SIFT-MS can only be used to estimate the concentration of *total* terpenes present in an air sample using H_3O^+ and NO^+ ions, with only limited capability to distinguish between paired terpene isomers.

Keywords: SIFT; Terpenes; Proton transfer; Charge transfer; SIFT-MS

---

1. Introduction

Terpenes and their oxygenated derivatives terpenoids are present in and emitted from many commonly available products such as fruits and fruit juices, spices and natural aromas [1,2]. Considerable effort has been given to their analysis in natural products, notably using gas chromatography mass spectrometry (GCMS), and to their isolation and synthesis for use as food flavours and as components of synthetic perfumes [2–4]. They are also important in atmospheric chemistry and known to be emitted from trees and especially from pine forests [5,6]. Our interest in these compounds follows our development of selected ion flow tube mass spectrometry (SIFT-MS) [7,8], which is a useful addition to the analytical methods available and which is valuable for real time quantitative analysis of volatile emissions from foods and food flavours [9]. In order to use SIFT-MS for trace gas analyses, the kinetics must be understood of the reactions of the trace species to be analysed with the commonly used precursor ions that are used for chemical ionisation in SIFT-MS [10]. The present study is

---

[*] Corresponding author. Tel.: +420-2-6605-2112;
fax: +420-2-858-2307.
E-mail address: spanel@seznam.cz (D. Smith).

1387-3806/03/$ – see front matter © 2003 Elsevier B.V. All rights reserved.
doi:10.1016/S1387-3806(03)00271-9

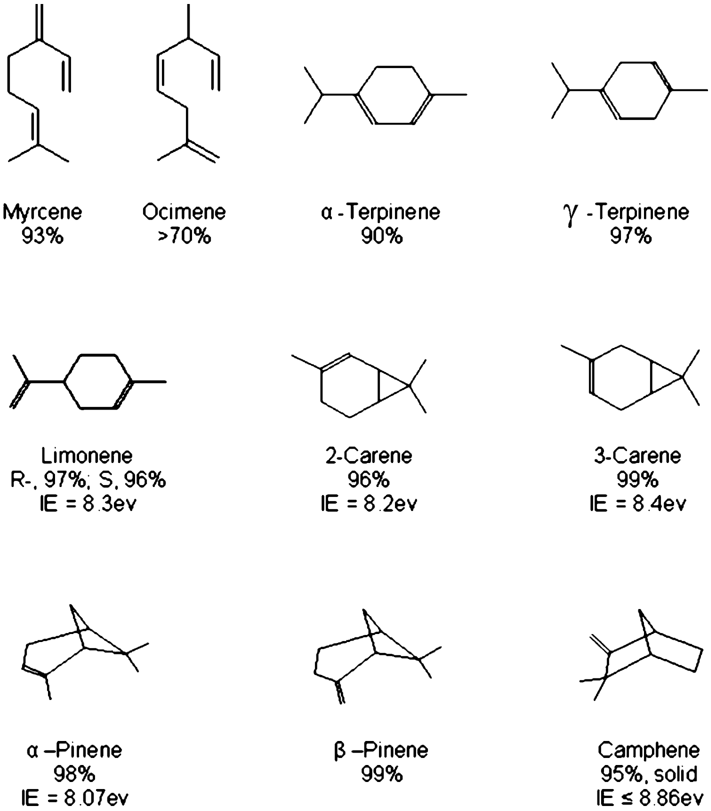

Scheme 1.

intended to supplement the understanding of the gas phase ion chemistry of monoterpenes and thus to extend our SIFT-MS database into this area of analysis.

Monoterpenes, $C_{10}H_{16}$, can be seen as a combination of two isoprene-like moieties, C_5H_8. Isoprene, 2-methyl butadiene, has a conjugated diene structure, $CH_2{=}C(CH_3)CH{=}CH_2$. It is emitted, together with some terpenes, by certain trees and plants [11] and interestingly is a component of the exhaled breath of humans [12]. Monoterpenes may be cyclic, acyclic, saturated or unsaturated as can be seen in Scheme 1. Their distinguishable isomers can differ only by as much as the positioning of a double bond within a ring (e.g., α- and γ-terpinene) and there exist optical isomers of some (e.g., limonene). In general, they are high boiling point oils, but they do have significant vapour pressures at room temperature, which allows the study of their gas phase chemistry. The terpenes included in this study are given in Scheme 1, where their structures are indicated. Only one of these, camphene, is solid at room temperature and to some extent this property is apparently reflected in its different ion chemistry (its propensity to form adducts), as we will see.

Much previous work has shown that these various monoterpenes can be isolated and identified using GCMS [13]. A major objective of the present study is to investigate if the rather subtle differences in the structures of these compounds can be recognised by ion chemistry and, if so, whether or not they are amenable to individual identification and quantification using SIFT-MS. As this study shows, this desirable objective can only be partially achieved and even then very careful SIFT-MS analyses are necessary. However, total terpenes in a sample may be analysed in real time using SIFT-MS with some confidence, which has its place in the analysis of natural products.

We have previously briefly investigated the reactions of H_3O^+, NO^+ and $O_2{}^+$ with limonene, and the terpenoids menthone [9] and menthol [14] as our entry to food flavour research. Other studies of the ion chemistry of these classes of compounds are limited to a very recent report of the ion chemistry of H_3O^+ with four terpenes, viz. α- and β-pinene, limonene, 3-carene, and the related compounds: *p*-cymene and camphor [15].

2. Experimental

The standard SIFT technique has been described in numerous publications [14,16,17] and so it is sufficient here to summarise it as follows. Precursor ions H_3O^+, NO^+ and $O_2{}^+$ are generated in a discharge ion source, mass selected by a quadrupole mass filter and then injected as selected ionic species into fast-flowing helium carrier gas in a flow tube. The reactant gases of interest (in these experiments, monoterpenes) are then introduced at controlled flow rates into the ion swarm/carrier gas where they react with the chosen precursor ion species. The loss rates of the precursor ions and the product ions of the reactions are determined by a downstream quadrupole mass spectrometer. This can be operated either in the full scan mode (FSM) over a predetermined *m*/*z* range to obtain a spectrum of the reactant and product ions or in the multi-ion mode (MIM) in which the spectrometer is switched and dwells on selected reactant/product ions as their count rates are determined [8]. The FSM is primarily used to identify the product ions and the MIM is used to accurately determine product ion distributions [8,10].

In these studies, the monoterpene vapours were introduced into the carrier gas as follows. A drop of the terpene liquid is introduced into a sealable plastic bag, which is then inflated using dry cylinder air (to a volume of about 500 mL). The liquid vapour/air mixture is then introduced into the helium carrier gas via a variable leak (needle valve) by puncturing the bag with a hypodermic needle connected to the inlet port of the instrument. Determination of the count rates of the precursor and product ions allows the rate coefficients and the product ion distributions to be deduced. Normally, the concentration of the liquid vapour in the air is unknown. So to determine the relative rate coefficients of the three precursor ion species with each terpene molecule, we compare the decay rates of the H_3O^+, NO^+ and $O_2{}^+$ ions, simultaneously injected into the carrier gas, as the flow rate of the dry air/sample mixture is varied. Details of this technique have been given in several papers (see, for example [16]). This particular method has been used exclusively in these studies. Additionally in the present studies, in order to support real SIFT-MS studies, the ion product distributions were determined under three circumstances: (i) using dry helium carrier gas, i.e., with only the dry air/terpene mixture entering the carrier gas, (ii) with laboratory air (relative humidity about 1.5%) also introduced into the carrier gas at a flow rate typical of that used for SIFT-MS analyses of ambient air and exhaled breath (2 Torr L s^{-1} [7,8]), (iii) with humid air (relative humidity about 6%) introduced at this same flow rate obtained above liquid water held near 310 K to simulate exhaled breath [18]. Clearly, these extra experiments were carried out to study the influence of air (N_2 and O_2) and water vapour on the observed product ion distributions.

To prevent condensation of water vapour and the terpenes onto the inlet lines, they are heated to about 100 °C. All the present studies were carried out at a helium carrier gas pressure of 0.7 Torr at room temperature (296–300 K).

3. Results

3.1. General comments

The limited amount of kinetic data available on the reactions of H_3O^+ ions with monoterpenes [9,15] show that they proceed at the gas kinetic rate. This indicates that the proton affinities (PA) of the monoterpenes exceed that of H_2O molecules ($\mathrm{PA}(H_2O) = 691\ \mathrm{kJ\,mol^{-1}}$). The only molecule with the molecular formula $C_{10}H_{16}$ with a known PA

Table 1
The measured rate coefficients, *k*, for the reactions of NO^+ and $O_2{}^+$ with the monoterpenes, with the common molecular formulae $C_{10}H_{16}$ and molecular weight of 136 Da

Molecule	*k* (NO^+)[a] ($10^{-9}\,cm^3\,s^{-1}$)	*k* ($O_2{}^+$)[a] ($10^{-9}\,cm^3\,s^{-1}$)
Myrcene	2.2	2.2
Ocimene	2.1	1.9
α-Terpinene	2.0	2.0
γ-Terpinene	2.1	1.9
R-Limonene	2.2	2.2
S-Limonene	2.0	1.9
2-Carene	2.3	2.0
3-Carene	2.2	1.9
α-Pinene	2.3	2.1
β-Pinene	2.1	2.0
Camphene	2.3	2.2

[a] On the assumption that all the H_3O^+ reactions proceed at the collisional rate ($k_c = 2.6 \times 10^{-9}\,cm^3\,s^{-1}$), the *k* for the NO^+ and $O_2{}^+$ reactions have been experimentally derived by the procedure described in Section 2. The estimated absolute and relative uncertainties in these calculated rate coefficients are ±25 and 15%, respectively.

is 3-methylene-1,5,5-trimethylcyclohexene; PA = 904.9 kJ mol^{-1} [19]. So it is safe to assume that the reactions with H_3O^+ of the monoterpenes included in this study proceed at the collisional rate (rate coefficient, k_c). This assumption is strongly supported by the fact that the relative decay rates of H_3O^+, NO^+ and $O_2{}^+$ ions in reaction with all the 11 terpenes are in accordance with the reduced mass of the reactant systems, as indicated by the rate coefficient values, *k*, given in Table 1. The value of k_c can be calculated if the polarisability and the dipole moment of the reactant terpene molecule is known, but unfortunately there are little such data available. So we have had to estimate these parameters by taking values that are available for similar molecules (see those given in [20]). Hence, we have adopted common values of the polarisabilities as $(17 \pm 2.0) \times 10^{-24}\,cm^3$ and the permanent dipole moments as (0.7 ± 0.15) Debye for all the $C_{10}H_{16}$ terpenes and used the theory of Su and Chesnavich [21] to calculate the common k_c values for the reactions of all 11 terpenes with the H_3O^+, NO^+ and $O_2{}^+$ precursor ions. Thus, $k_c\ (H_3O^+) = 2.6 \times 10^{-9}\,cm^3\,s^{-1}$, $k_c\ (NO^+) = 2.1 \times 10^{-9}\,cm^3\,s^{-1}$, $k_c\ (O_2{}^+) = 2.1 \times 10^{-9}\,cm^3\,s^{-1}$. Since $k = k_c$ for the H_3O^+ exothermic proton transfer reactions, the relative decay rates of the three precursor ions provides *k* values for the NO^+ and $O_2{}^+$ reactions (which a priori cannot be assumed to proceed at their collisional rates). Thus, as can be seen in Table 1, all 33 reactions proceed at or close to their respective collisional rates. We now discuss the product ion distributions for these reactions.

3.2. H_3O^+ reactions

Only two of the 11 terpenes, M, included in this study are acyclic, these being myrcene and ocimene (see Scheme 1). The reactions of all these terpenes with H_3O^+ apparently proceed via exothermic proton transfer (but see the reaction mechanism later). Partial dissociation of the nascent $(MH^+)^*$ product ions occurs, but in all 11 reactions MH^+ ions, i.e., $C_{10}H_{17}{}^+$, are the major product ions with $C_6H_9{}^+$ ions being the major fragment ion, as can be seen in Table 2. This agrees with the four observations reported in [15] and the data for limonene that we reported earlier [9]. No significant differences in the product distributions are observed when atmospheric air (relatively low humidity) is introduced into the helium carrier gas, which simplifies the analysis of terpenes in ambient air. However, on the addition of humid air, a product ion appears at a *m*/*z* value of 155, variously at the 1–3% level, which is the hydrated ion $C_{10}H_{17}{}^+H_2O$. What at first sight was surprising is that with the appearance of these hydrates the percentages of the $C_{10}H_{17}{}^+$ ions tend to decrease while the fragment ions increase somewhat (see Table 2). These observations give a clue as to the mechanism of these reactions. Thus, the presence of the water molecules results in a decrease in the fragmentation channels and in additional hydration. Therefore, we tentatively propose that these reactions proceed first by the formation of $(H_3O^+M)^*$ excited ions, which are more effectively quenched in collisions with H_2O molecules. This results in a decrease in the internal energy of the transient ion (fractionally more stabilisation), which results in less fragmentation and also some stable H_3O^+M, i.e.,

Table 2
The percentage product ion distributions for the reactions of H_3O^+ with terpenes

Terpene	$C_6H_9^+$ ($m/z = 81$)			$C_{10}H_{17}^+$ ($m/z = 137$)[a]			Minority ions (typical percentages, %)
	NA	LA	MA	NA	LA	MA	
Myrcene	30	30	26	57	58	64	$C_5H_9^+$ (3), $C_7H_{11}^+$ (9)
Ocimene	27	24	21	62	65	70	$C_4H_9^+$ (3), $C_5H_9^+$ (3), $C_7H_{11}^+$ (4)
α-Terpinene	11	10	9	86	87	88	$C_{10}H_{15}^+$ (3)
γ-Terpinene	18	17	13	80	81	84	$C_{10}H_{15}^+$ (3)
R-Limonene	30	29	25	67	68	72	$C_7H_{11}^+$ (3)
S-Limonene	31	30	25	66	67	73	$C_7H_{11}^+$ (3)
2-Carene	19	18	14	81	82	86	–
3-Carene	25	24	19	75	76	81	–
α-Pinene	38	39	38	62	61	62	–
β-Pinene	43	40	34	57	60	66	–
Camphene	15	14	12	85	86	88	–

NA: no air, LA: lab air, MA: moist air, (–) this means there are no significant minority product ions at the particular *m/z* values.

[a] $C_{10}H_{17}^+H_2O$ ions at $m/z = 155$ are at the 1–3% level in all reactions. These have been rolled into the $C_{10}H_{17}^+$ at $m/z = 137$ percentages.

MH^+H_2O, ions:

$$H_3O^+ + C_{10}H_{16} + He \rightarrow (H_3O^+C_{10}H_{16})^{**} + He \quad (1a)$$

$$(H_3O^+C_{10}H_{16})^{**} + H_2O \rightarrow (H_3O^+C_{10}H_{16})^{*} + H_2O \quad (1b)$$

$$(H_3O^+C_{10}H_{16})^{**} + H_2O \rightarrow H_3O^+H_2O + C_{10}H_{16} \quad (1c)$$

$$(H_3O^+C_{10}H_{16})^{*} \rightarrow (C_{10}H_{17}^+ + H_2O) + (C_6H_9^+ + C_4H_7) + C_{10}H_{17}^+H_2O \quad (1d)$$

The most controversial step in this scenario is the proposal that formation of the $(H_3O^+C_{10}H_{16})^{**}$ ion occurs rather than the reaction proceeding via direct spontaneous proton transfer. But there is precedence for association reactions like (1a). We have previously observed that adduct ions do indeed form in the reactions of long chain alkanes with H_3O^+ [22]. For example, the reaction of H_3O^+ with dodecane proceeds at the collisional rate to form $H_3O^+C_{12}H_{26}$ adducts. However, in the presence of water molecules the following rapid switching reaction occurs:

$$H_3O^+C_{12}H_{26} + H_2O \rightarrow H_3O^+H_2O + C_{12}H_{26} \quad (2)$$

In effect, the presence of the dodecane catalyses the production of the $H_3O^+H_2O$ ions. It is significant in the present terpene experiments that some formation of $H_3O^+H_2O$ ions is seen in the relatively dry helium carrier gas with the introduction of the terpene molecules. Hence, the reason for the inclusion of reaction (1c) in the reaction scheme given above, although this is only a very minor channel (<1%).

A further interesting observation is that $H_3O^+H_2O$ ions react rapidly with these terpene molecules. This we were able to show by directly injecting these ionic species as precursors into the helium carrier gas. Unfortunately, upon injection, the large fraction of these weakly bound ions (>90%) dissociated in collisions with the helium atoms to give H_3O^+, so the product ion distributions of the $H_3O^+H_2O$/terpenes reactions could not be completely distinguished from the products of the H_3O^+ reactions. However, careful analysis of the data indicates that the non-dissociated protonated molecules $C_{10}H_{17}^+$ are the major products, i.e., no fragmented hydrocarbon ions are produced. This is consistent with the smaller amount of energy available as compared to the H_3O^+ reaction when the reaction proceeds via proton transfer thus:

$$H_3O^+H_2O + C_{10}H_{16} \rightarrow (C_{10}H_{17}^+)^* + 2H_2O \quad (3)$$

All these reactions proceed rapidly, which implies that the PA of these terpenes exceed the sum of PA(H_2O) 691 kJ mol^{-1} [19] and the binding energy of H_2O to H_3O^+, which is 133 kJ mol^{-1}, i.e., PA(terpenes) are greater than 824 kJ mol^{-1}. It is worthy of note that $H_3O^+H_2O$ ions proton transfer to isoprene molecules (C_5H_8) [23], which have a PA of 826 kJ mol^{-1} [19]. Strictly speaking, the two water molecules produced in reaction (3) could be formed initially as a neutral water dimer, thus contributing its binding energy of 21 kJ mol^{-1} [24] to the reaction energetics, but there is no precedence for such a process as far as we know.

There are measurable differences between the product distributions for the differing structural isomers but not, as expected, for the two optical isomers of limonene, which are essentially identical, as a glance at Table 2 shows. These limonene data also show the remarkable accuracy of these SIFT measurements for data taken at quite different times. Note that $C_7H_{11}^+$ (+C_3H_5 radicals) are minor products of the limonene reactions. Of the other cyclic terpenes, an additional minor product ion (at the 3% level) is observed in the terpinene reactions only. Presumably, this is due to the process of dissociative proton transfer (H_2 loss) shown as reaction (4c):

$$H_3O^+ + \alpha\text{- and }\gamma\text{-terpinene}$$

$$\rightarrow C_{10}H_{17}^+ + H_2O \qquad (4a)$$

$$\rightarrow C_6H_9^+ + C_4H_7 + H_2O \qquad (4b)$$

$$\rightarrow C_{10}H_{15}^+ + H_2 + H_2O \qquad (4c)$$

Loss of H_2 from the protonated molecule is relatively uncommon for H_3O^+ reactions, but not unknown [25]. Its product ion is identical to that which would result from hydride ion transfer, a process that is common in NO^+ reactions [26]. Indeed, this obviously occurs in some of the NO^+/terpene reactions included in the present study (see Table 2).

A glance at Table 2 shows that there appear additional minor product channels for the two acyclic molecules myrcene and ocimene. The smaller product ions $C_4H_9^+$ and $C_5H_9^+$ appear, showing that the protonated molecule splits along the carbon skeletons.

3.3. NO^+ reactions

The recombination energy of ground state NO^+ ions is 9.26 eV [27]. The ionisation energies of polyatomic hydrocarbon molecules, including the terpenes, are generally less than this value (e.g., that of α-pinene is 8.07 eV [27]). So it is no surprise to find that charge transfer occurs in all of these NO^+/terpene reactions:

$$NO^+ + C_{10}H_{16} \rightarrow C_{10}H_{16}^+ + NO \qquad (5)$$

Indeed, the parent cations, $C_{10}H_{16}^+$, are the major product ions in all 11 reactions, as can be seen in Table 3. However, the exothermicity of these charge transfer reactions is insufficient to allow dissociative charge transfer to occur and so the fragment ions that appear as products in these NO^+ reactions must be produced by processes other than charge transfer. The most obvious processes are H^- and R^- abstraction (R = CH_3, C_2H_3, C_3H_6, C_3H_7, C_3H_8, etc.), clearly exemplified in the γ-terpinene reaction (see Table 3):

$$NO^+ + C_{10}H_{16} \rightarrow C_{10}H_{16}^+ + NO \qquad (6a)$$

$$\rightarrow C_{10}H_{15}^+ + HNO \qquad (6b)$$

$$\rightarrow C_7H_9^+ + (NOC_3H_7) \qquad (6c)$$

$$\rightarrow C_7H_8^+ + (NOC_3H_8) \qquad (6d)$$

The dominant charge transfer reaction (6a) occurs in parallel with the other abstraction reactions in which the neutral products are HNO and NOR molecules, as indicated. This process is quite common in the reactions of NO^+ ions with other hydrocarbons [22] and other types of organic molecules, including ethers [28], carboxylic acids and esters [29]. The most obvious difference in these product ion distributions between paired isomers is the clear occurrence of H^- abstraction in the γ-terpinene reaction (6b), which is hardly apparent in the analogous α-terpinene reaction (see Table 3). Less fragmentation also occurs in the α-terpinene reaction and this is presumably due to the

Table 3
The percentage product ion distributions for the reactions of NO^+ with terpenes

Terpene	$C_7H_8^+$ ($m/z = 92$)			$C_7H_9^+$ ($m/z = 93$)			$C_{10}H_{16}^+$ ($m/z = 136$)[a]			Minority ions (typical percentages, %)
	NA	LA	MA	NA	LA	MA	NA	LA	MA	
Myrcene	11	11	11	44	34	33	45	55	56	–
Ocimene	29	29	32	22	16	13	49	55	55	–
α-Terpinene	–	–	–	–	–	–	99	99	98	$C_{10}H_{15}^+$ (1)
γ-Terpinene	3	3	1	9	3	2	75	75	76	$C_{10}H_{15}^+$ (18)
R-Limonene	5	3	3	4	1	1	82	89	90	$C_7H_{10}^+$ (2), $C_9H_{13}^+$ (2), $C_{10}H_{15}^+$ (4)
S-Limonene	7	3	2	4	2	1	80	90	91	$C_7H_{10}^+$ (3), $C_9H_{13}^+$ (2), $C_{10}H_{15}^+$ (3)
2-Carene	–	–	–	2	–	–	98	100	100	–
3-Carene	12	7	7	14	8	4	71	81	84	$C_{10}H_{15}^+$ (4)
α-Pinene	26	16	14	18	7	6	56	77	80	–
β-Pinene	6	4	2	19	7	5	75	89	93	–
Camphene [b]	2	2	0	3	1	2	69	79	79	$C_7H_{10}^+$ (2), $C_9H_{13}^+$ (9), $NO^+C_{10}H_{16}$ (11)[b]

NA: no air, LA: lab air, MA: moist air, (–) this means there are no significant minority product ions at the particular *m/z* values.

[a] $NO^+C_{10}H_{16}$ ions at $m/z = 166$ are at the 1–3% level in all reactions except for camphene (see table footnote b). These product ions have been rolled into the $C_{10}H_{16}^+$ at $m/z = 136$ percentages.

[b] For camphene, $C_9H_{13}^+$ and $NO^+C_{10}H_{16}$ are both significant products and their percentages differ for the no air situation and when air is present. $C_9H_{13}^+$ (16), $NO^+C_{10}H_{16}$ (9) for no air; $C_9H_{13}^+$ (5), $NO^+C_{10}H_{16}$ (10) for lab air; and $C_9H_{13}^+$ (5), $NO^+C_{10}H_{16}$ (13) for moist air.

greater stability of α-terpinene imparted by the conjugated double bonds (see the structures in Scheme 1).

It is noticeable that the fraction of the parent cations at $m/z = 136$ in the product distributions for all of these terpene reactions increases as the air/water is introduced into the helium, perhaps implying some "quenching" of the nascent $(M^+)^*$ excited ions by N_2 and O_2 molecules. This would presumably result in less fragmentation. However, an alternative explanation is that the minor fragment product ions are reactive with H_2O molecules.

A product ion at a *m/z* value of 166 appears in most of these reactions, but this adduct is only minor at the 1–3% level except for the camphene reaction where it is at the 10% level (see Table 3). It is clear that the percentages of these ions increase when laboratory air

Table 4
The percentage product ion distributions for the reactions of O_2^+ with terpenes

Terpene	$C_7H_8^+$ ($m/z = 92$)			$C_7H_9^+$ ($m/z = 93$)			$C_9H_{13}^+$ ($m/z = 121$)			$C_{10}H_{16}^+$ ($m/z = 136$)			Minority ions (typical percentages, %)
	NA	LA	MA	NA	LA	MA	NA	LA	MA	NA	LA	MA	
Myrcene	69	70	71	5	5	4	6	7	6	3	3	3	$C_5H_9^+$ (10), $C_6H_8^+$ (3), $C_7H_{10}^+$ (5)
Ocimene	10	9	9	47	45	45	19	18	18	3	7	5	$C_5H_8^+$ (4), $C_6H_8^+$ (6), $C_7H_{10}^+$ (5), $C_8H_{11}^+$ (7)
α-Terpinene	4	4	4	16	16	14	41	42	40	33	33	36	$C_8H_{11}^+$ (3)
γ-Terpinene	12	12	11	49	46	45	21	21	22	11	14	14	$C_6H_8^+$ (3), $C_8H_{11}^+$ (4)
R-Limonene	8	10	8	31	30	29	12	13	14	11	11	11	$C_5H_8^+$ (10), $C_6H_8^+$ (5), $C_7H_{10}^+$ (12), $C_8H_{11}^+$ (11)
S-Limonene	9	8	9	29	32	29	15	13	13	10	9	11	$C_5H_8^+$ (9), $C_6H_8^+$ (4), $C_7H_{10}^+$ (12), $C_8H_{11}^+$ (11)
2-Carene	2	3	4	21	19	17	50	48	50	19	22	21	$C_8H_{11}^+$ (4)
3-Carene	11	11	11	45	45	45	19	20	20	9	9	10	$C_6H_8^+$ (8), $C_7H_{10}^+$ (2), $C_8H_{11}^+$ (4)
α-Pinene	21	22	21	56	56	57	13	12	12	4	5	4	$C_6H_8^+$ (3), $C_8H_{11}^+$ (3)
β-Pinene	6	6	6	64	64	65	9	10	9	9	9	10	$C_5H_9^+$ (3), $C_6H_8^+$ (4), $C_8H_{11}^+$ (3)
Camphene	5	4	5	18	19	16	47	49	51	9	9	8	$C_6H_8^+$ (2), $C_8H_{11}^+$ (10), $C_8H_{12}^+$ (6)

NA: no air, LA: lab air, MA: moist air, (–) means there are no significant minority product ions at the particular *m/z* values.

and moist air are added to the helium. This gives a clue as to the origin of this minority product ion, because on the addition of the water vapour ions at a *m/z* value of 48 appear, these being NO^+H_2O ions [30]. These ions are formed via three-body association of the NO^+ precursor ions with H_2O molecules:

$$NO^+ + H_2O + He \rightarrow NO^+H_2O + He \tag{7}$$

The relative count rates of the NO^+H_2O to NO^+ ions increases as the number density of the H_2O molecules in the helium carrier gas increases, being about 1/20 when the moist is introduced. This is typical of the situation that arises when exhaled breath is introduced and so when breath analysis is being performed, the presence of these NO^+H_2O ions must be accounted for [10]. Hence, we are currently carrying out a thorough study of the reactions of these NO^+ hydrated ions. They are reactive with a range of organic compounds, common reaction processes being ligand switching and charge transfer, i.e.,

$$NO^+H_2O + \text{terpene} \rightarrow NO^+(\text{terpene}) + H_2O \tag{8}$$

$$NO^+H_2O + \text{terpene} \rightarrow \text{terpene}^+ + (NO + H_2O) \tag{9}$$

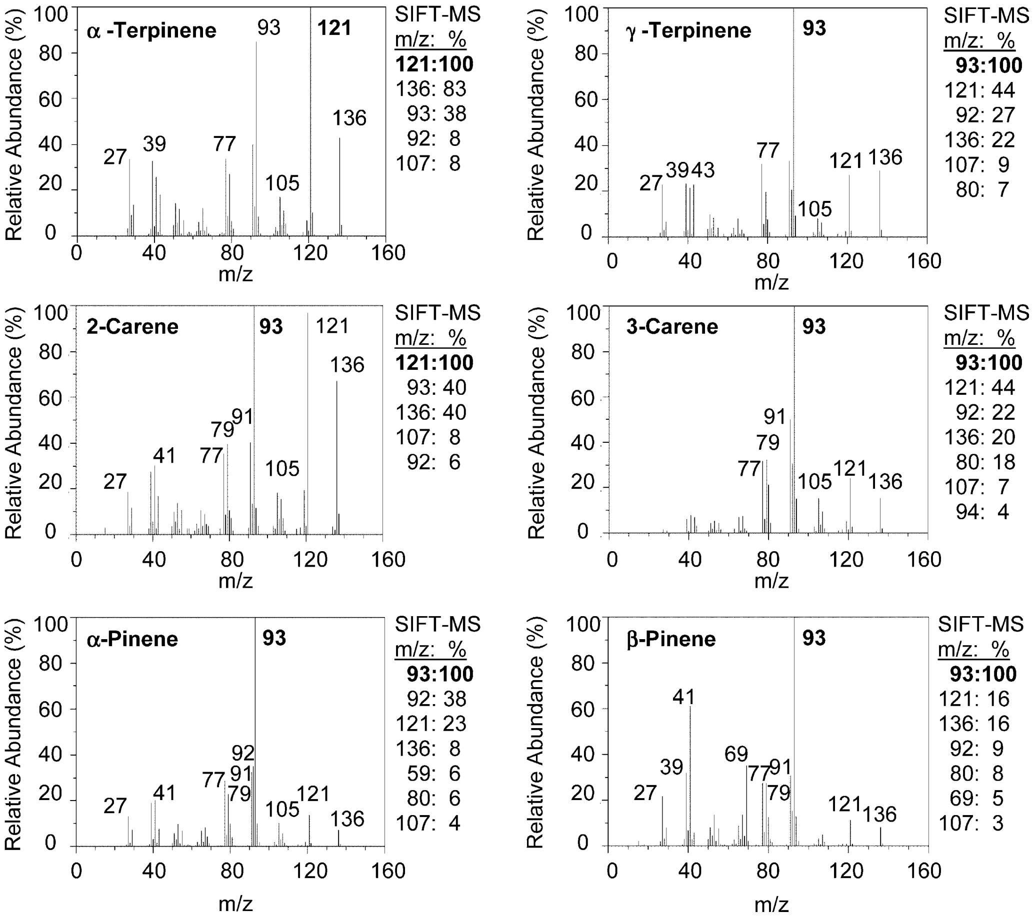

Fig. 1. Comparison of the electron impact (EI) spectra obtained using 70 eV electron [33] for six selected terpenes, α- and γ-terpinene, 2- and 3-carene, and α- and β-pinene, with the product ion distributions of the corresponding O_2^+ reactions, which have been normalised to the most abundant ion as in the respective EI spectra. In these EI spectra the parent cations are minor species, but more product ions are apparent in these spectra with more low mass ions than are produced in the O_2^+ reactions.

The switching process is partly responsible for the production of the ions at *m*/*z* values at 166 in these terpene reactions, the other process being three-body association of NO^+ with the terpene molecules, analogous to reaction (7). That these switching reactions (8) occur rapidly indicates that the NO^+–terpene binding energies exceed that of NO^+–H_2O which is known to be about 0.7 eV [31,32]. The charge transfer reactions (9) are energetically allowed when the ionisation energy (IE) of the terpene molecule is less than that of NO molecules minus the NO^+–H_2O binding energy. Thus, the IE(terpene) must be less than $(9.26 - 0.7) = 8.56$ eV, which is certainly the case for limonene (IE = 8.3 eV), α-pinene (8.07 eV), 2-carene (8.2 eV), 3-carene (8.4 eV) but, perhaps significantly, not for camphene (≤8.86 eV) in which reaction the greatest fraction of the adduct ion appears (these IE values are taken from [27]). Thus, these two processes (8) and (9) are effectively competing in these NO^+H_2O/terpene reactions.

3.4. $O_2{}^+$ reactions

As expected from much previous work on the reactions of $O_2{}^+$ ions, there appear more fragment ions than in the H_3O^+ and NO^+ reactions, as can be seen in Table 4. This is due to the relatively large recombination energy of $O_2{}^+$ ions, which is 12.2 eV [27]. Thus, in contrast with the NO^+ reactions, the parent cations $C_{10}H_{16}{}^+$ are not the major product ions in any of these terpene reactions. It is instructive to compare these product ion distributions with the “fragmentation patterns” obtained using 70 eV electrons, i.e., the electron impact (EI) spectra that are published for 9 of the 11 terpenes included in this study [33]. In these EI spectra the parent cations are also minor species, but considerably more product ions are apparent than in the $O_2{}^+$ reactions with a greater fraction of low mass ions. Comparisons of the EI spectra with the product ions of the $O_2{}^+$ reactions are shown in Fig. 1. It is clear that there appear two major product ions in both the SIFT and the EI spectra, these being $C_7H_9{}^+$ and $C_9H_{13}{}^+$ ions at *m*/*z* values at 93 and 121, respectively, showing that the ejection of C_3H_7 and CH_3 radicals from the nascent $(C_{10}H_{16}{}^+)^*$ is facile.

It is interesting and potentially useful for analyses that there are clear differences in both the SIFT and EI product ion spectra for the paired isomers, as can be seen in Fig. 1. Note the prominence of $m/z = 93$ in all the EI spectra and most of the $O_2{}^+$ data and the prominence of $m/z = 121$ for α-terpinene and 2-carene $O_2{}^+$ data.

4. Concluding remarks

All the 33 reactions studied here proceed at the collisional rate, which facilitates the analyses of these terpenes using SIFT-MS, but less satisfactorily is that the reactions mostly result in multiple ion products, which complicates SIFT-MS analyses. The use of $O_2{}^+$ precursor ions for SIFT-MS analyses of terpenes is impractical because of the multiple product ions. The best that can be achieved is to analyse *total* terpenes, using the sums of the product ions at *m*/*z* of 81 and 137 using H_3O^+ precursors and 136 and 93 using NO^+ precursors, but then only to an accuracy of about a factor of 2. Distinguishing between paired isomers is also difficult. However, when specific monoterpenes are known to be present in a sample, the use of NO^+ precursor ions may be used to distinguish between the terpinene, carene and pinene paired isomers, as can be seen by scrutinising the ion distributions shown in Table 3. Notwithstanding these conclusions, this study has provided a good deal of fundamental data on the reactions of monoterpenes with the three very different ions, indicating that a range of processes occur and providing some information on the mechanisms of these complex reactions.

Acknowledgements

We thank Edward Hall and Ann Diskin for their help with the experiments. We gratefully acknowledge financial support by the Engineering and Physical Sciences Research Council, UK (grant reference GR/M89195/01) and the Grant Agency of the Czech

Republic (projects 202/03/0827 and 203/02/0737). We also thank the R.C. Treatt & Co. Ltd. for providing us with a sample of ocimene.

References

[1] A. Pabst, D. Barron, P. Etievant, P. Schreier, J. Agric. Food Chem. 39 (1991) 173.
[2] J.J. Mateo, M. Jimenez, J. Chromatogr. A 881 (2000) 557.
[3] G. Krammer, P. Winterhalter, M. Schwab, P. Schreier, J. Agric. Food Chem. 39 (1991) 778.
[4] M.D. Guillen, N. Cabo, J. Burillo, J. Sci. Food Agric. 70 (1996) 359.
[5] G. Konig, M. Brunda, H. Puxbaum, C.N. Hewitt, S.C. Duckham, J. Rudolph, Atmos. Environ. 29 (1995) 861.
[6] R.W. Janson, J. Geophys. Res. Atmos. 98 (1993) 2839.
[7] D. Smith, P. Španěl, Int. Rev. Phys. Chem. 15 (1996) 231.
[8] P. Španěl, D. Smith, Med. Biol. Eng. Comput. 34 (1996) 409.
[9] P. Španěl, D. Smith, Rapid Commun. Mass Spectrom. 13 (1999) 585.
[10] D. Smith, A.M. Diskin, Y. Ji, P. Španěl, Int. J. Mass Spectrom. 209 (2001) 81.
[11] J.W. Janson, J. Geophys. Res. 98 (1993) 2839.
[12] P. Španěl, S. Davies, D. Smith, Rapid Commun. Mass Spectrom. 13 (1999) 1733.
[13] B. Larsen, T. Bomboi-Mingarro, E. Brancaleoni, et al., Atmos. Environ. 31 (Suppl. 1) (1997) 35.
[14] D. Smith, N.G. Adams, Adv. Atom. Mol. Phys. 24 (1987) 1.
[15] A. Tani, S. Hayward, C.N. Hewitt, Int. J. Mass Spectrom. 223/224 (2003) 561.
[16] P. Španěl, D. Smith, Int. J. Mass Spectrom. Ion Process. 167/168 (1997) 375.
[17] P. Španěl, J.M. Van Doren, D. Smith, Int. J. Mass Spectrom. 213 (2002) 163.
[18] D. Smith, P. Španěl, Rapid Commun. Mass Spectrom. 15 (2001) 563.
[19] E.P. Hunter, S.G. Lias, J. Phys. Chem. Ref. Data 27 (1998) 413.
[20] D.R. Lide (Ed.), CRC Handbook of Chemistry and Physics, CRC, Boca Raton, FL, 1991.
[21] T. Su, W.J. Chesnavich, J. Chem. Phys. 76 (1982) 5183.
[22] P. Španěl, D. Smith, Int. J. Mass Spectrom. 181 (1998) 1.
[23] P. Španěl, D. Smith, J. Phys. Chem. 99 (1995) 15551.
[24] M.W. Feyereisen, D. Feller, D.A. Dixon, J. Phys. Chem. 100 (1996) 2993.
[25] P. Španěl, D. Smith, Int. J. Mass Spectrom. 176 (1998) 203.
[26] P. Španěl, D. Smith, J. Chem. Phys. 104 (1996) 1893.
[27] S.G. Lias, in: W.G. Mallard, P.J. Linstrom (Eds.), Ionization Energy Evaluation in NIST Chemistry WebBook, NIST Standard Reference Database Number 69, National Institute of Standards and Technology, Gaithersburg, MD, 2000.
[28] P. Španěl, D. Smith, Int. J. Mass Spectrom. Ion Process. 172 (1998) 239.
[29] P. Španěl, D. Smith, Int. J. Mass Spectrom. Ion Process. 172 (1998) 137.
[30] P. Španěl, D. Smith, Rapid Commun. Mass Spectrom. 14 (2000) 646.
[31] G. De Petris, A. Di Marzio, F. Grandinetti, J. Phys. Chem. 95 (1991) 9782.
[32] J.S. Francisco, J. Chem. Phys. 115 (2001) 2117.
[33] W.G. Mallard, P.J. Linstrom (Eds.), NIST Mass Spec Data Center, S.E. Stein, Director, IR and Mass Spectra in NIST Chemistry WebBook, NIST Standard Reference Database Number 69, National Institute of Standards and Technology, Gaithersburg, MD, 2000.